

Five-Field Peeling-Ballooning Modes Simulation and Differencing Schemes Analysis with BOUT++ Code



Tianyang Xia^{1,2}, Xueqiao Xu², Ben Dudson³ and Jangang Li¹

¹Institute of Plasma Physics, Chinese Academy of Sciences, Hefei, China.

²Lawrence Livermore National Laboratory, Livermore, CA 94550, USA

³University of York, Heslington, York YO10 5DD, United Kingdom





Theoretical Equations



$$\frac{\partial n_i}{\partial t} + \mathbf{V}_E \cdot \nabla n_i = 0,$$

$$\varpi = n_{i0} \frac{m_i}{B_0} \left[\nabla_{\perp}^2 \phi + \frac{1}{n_{i0}} \nabla_{\perp} \phi \cdot \nabla_{\perp} n_{i0} + \frac{1}{n_{i0} Z_i e} \nabla_{\perp}^2 p \right],$$

$$\frac{\partial T_j}{\partial t} + \mathbf{V}_E \cdot \nabla T_j = \nabla_{\parallel} (\kappa_{\parallel j} \nabla_{\parallel} T_j),$$

$$J_{\parallel} = J_{\parallel 0} - \frac{1}{\mu_0} \nabla_{\perp}^2 (B_0 \psi),$$

$$\frac{\partial}{\partial t} \varpi + \mathbf{V}_E \cdot \nabla \varpi = B_0 \mathbf{b} \cdot \nabla \frac{J_{\parallel}}{B_0} + 2 \mathbf{b} \times \boldsymbol{\kappa} \cdot \nabla P,$$

$$\mathbf{V}_E = \frac{1}{B_0} (\mathbf{b}_0 \times \nabla_{\perp} \Phi),$$

$$\frac{\partial \psi}{\partial t} = -\frac{1}{B_0} \mathbf{b} \cdot \nabla \Phi + \frac{\eta}{\mu_0} \nabla_{\perp}^2 \psi - \frac{\eta_H}{\mu_0} \nabla_{\perp}^4 \psi,$$

$$P = k_B n (T_i + T_e) = P_0 + p,$$

$$\Phi = \Phi_0 + \phi.$$



Linear growth rate for constant n_0



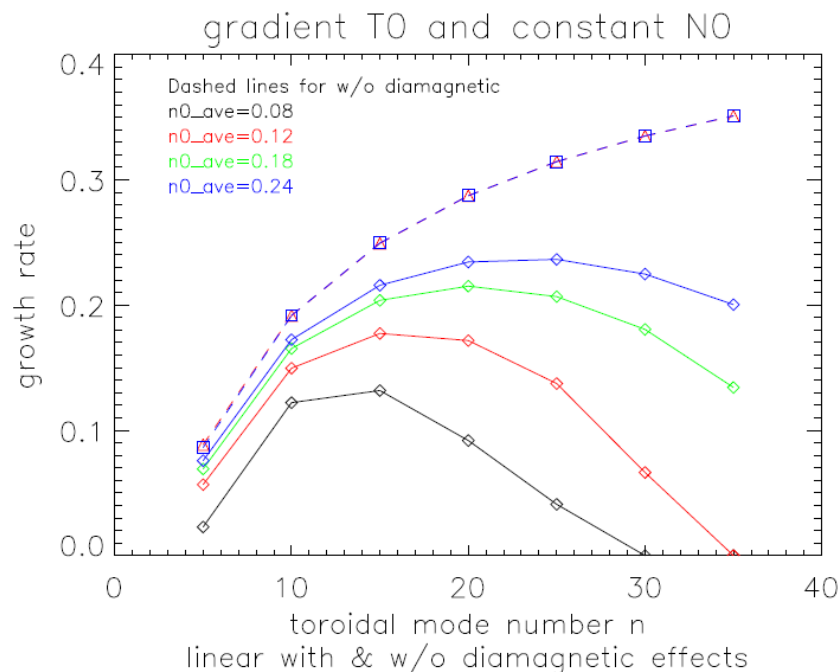
For Ideal MHD, constant n_0 is equivalent to the former 3-field results because the density terms do not appear in ideal MHD.

The frequency of perturbation is written as

$$\omega^2 + \omega \frac{1}{n_{i0} Z_{ie}} (\mathbf{b}_0 \times \mathbf{k} \cdot \nabla P_0) = \frac{2}{k_{\perp}^2 n_{i0}} (\mathbf{b}_0 \times \mathbf{k} \cdot \nabla P_0) (\mathbf{b}_0 \times \mathbf{k} \cdot \mathbf{k}) + \frac{B_0^2 k_{\parallel}^2}{n_{i0}} - \frac{B_0^2 k_{\parallel} (\mathbf{b}_0 \times \mathbf{k} \cdot \nabla J_{\parallel 0})}{n_{i0} k_{\perp}^2}.$$

$$\frac{\gamma_{nd}^2}{\omega_A^2} = \frac{\gamma_{nc}^2}{\omega_A^2} + i \frac{\gamma_{nd}}{\omega_A} \frac{1}{\sqrt{n_{i0} Z_{ie}}} (\mathbf{b}_0 \times \mathbf{k} \cdot \nabla P_0)$$

The diamagnetic drift term is just an oscillation. So the linear growth rate is inversely proportional to n_0 .



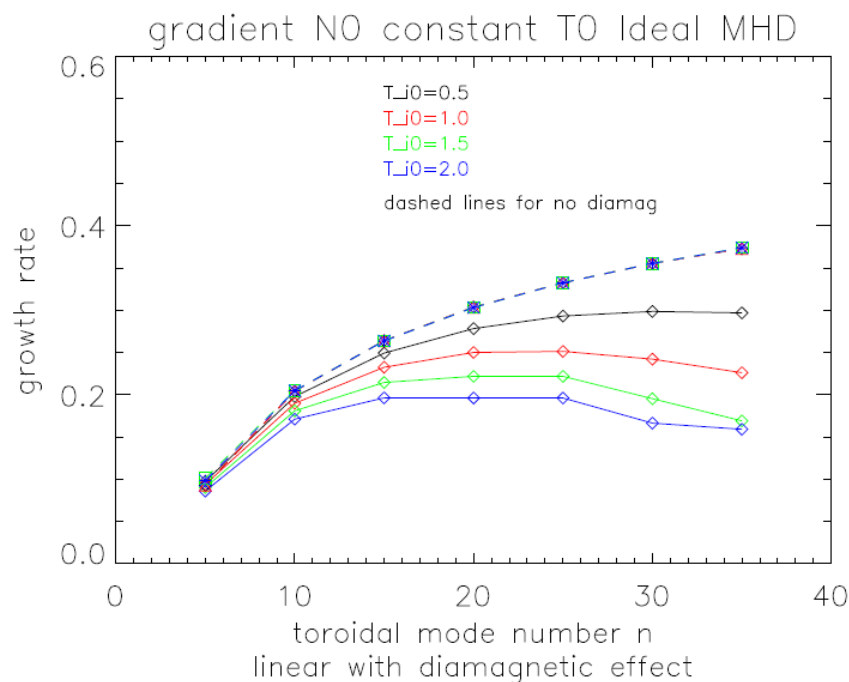


Linear growth rate for constant T_0



If T_0 is constant, then the cross terms in the Laplace equation for vorticity generate novel effects.

- For Ideal MHD, the cross term just acts as an oscillatory term, so for this case, the linear growth rate should not change a lot.
- With diamagnetic effects, the linear growth rate is inversely proportional to n_0 .





General cases for both gradient n_0 and T_0



For more general situation, both the equilibrium temperature and density profiles are not constant in the radial direction. Here we still apply the same pressure profile, but introduce a profile for ion density:

$$n_{i0}(x) = \frac{(n_{0_{height}} \times n_{ped})}{2} \left[1 - \tanh \left(\frac{x - x_{ped}}{\Delta x_{ped}} \right) \right] + n_{0_{ave}} \times n_{ped},$$

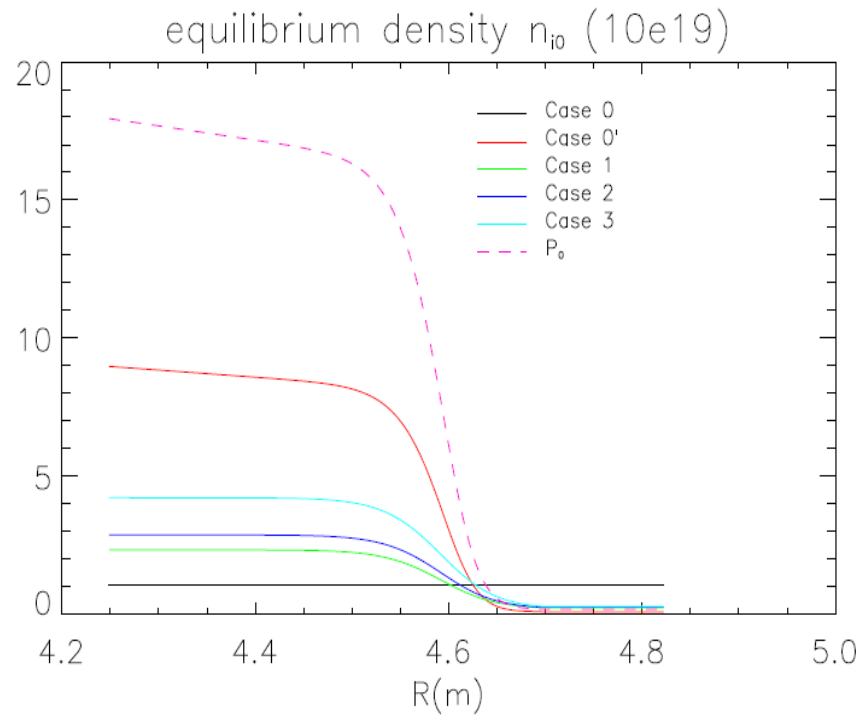
There are 5 density profiles are applied in this work:

	$n_{0_{ave}}$	$n_{0_{height}}$	$n_{0_{bot}} (\times 10^{19})$	$n_{0_{top}} (\times 10^{19})$	$n_{0_{ped-top}} (\times 10^{19})$
Case 0	0.12	0	1.00	1.00	1.00
Case 0'	-	-	0.09	8.97	3.98
Case 1	0.02	0.24	0.24	2.33	1.00
Case 2	0.02	0.30	0.25	2.87	1.29
Case 3	0.02	0.45	0.29	4.22	2.18

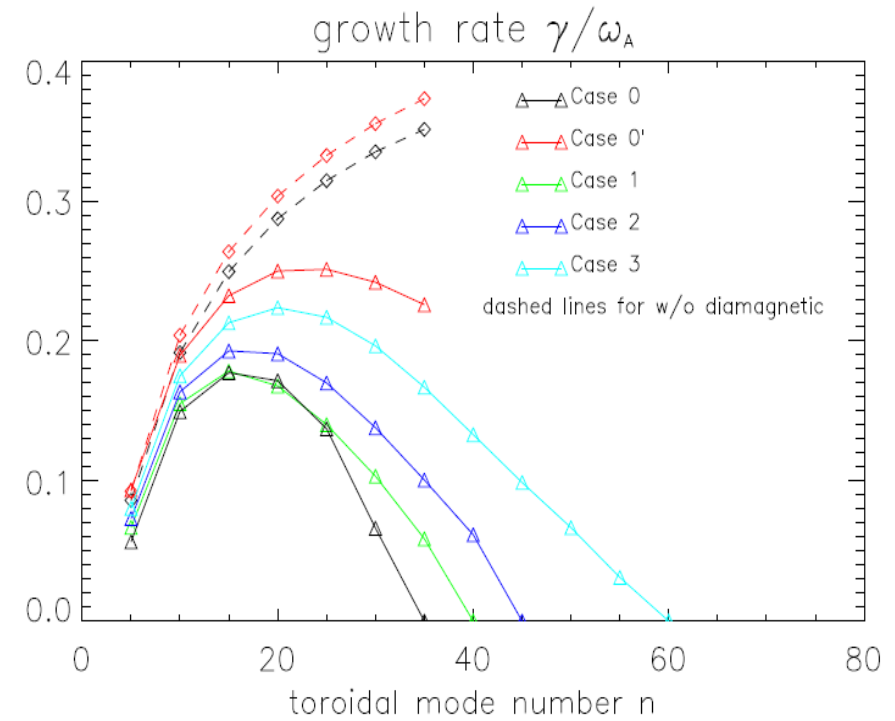
Table 1. The parameters of five models of different equilibrium ion density profile.



Linear growth rate for both gradient n_0 and T_0



The equilibrium density profiles for the cases in Table 1.



The linear growth rate for the cases in table 1. For Ideal MHD model, the linear growth rate of case 0' is larger than case 0 by 6.2%. With diamagnetic effects, the percentage goes to 31.43% for $n=15$



Why non-constant n_0 can enlarge γ



For constant T_0 , the Fourier analysis will give the angular frequency as:

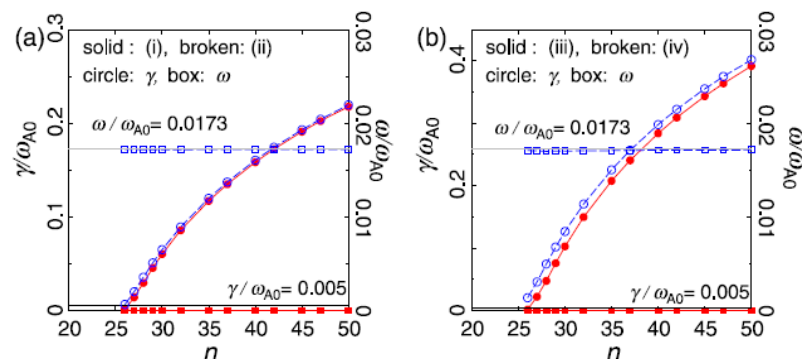
$$\begin{aligned}\omega_{Tc}^2 &= \left[\frac{2}{k_{\perp}^2 n_{i0}} (\mathbf{b}_0 \times \mathbf{k} \cdot \nabla P_0) (\mathbf{b}_0 \times \mathbf{k} \cdot \nabla J_{\parallel 0}) \right. \\ &\quad \left. + \frac{B_0^2 k_{\parallel}^2}{n_{i0}} - \frac{B_0^2 k_{\parallel} (\mathbf{b}_0 \times \mathbf{k} \cdot \nabla J_{\parallel 0})}{n_{i0} k_{\perp}^2} \right] \frac{1}{1 + i \frac{1}{k_{\perp} L_n}} \\ &= \frac{1}{1 + i \frac{1}{k_{\perp} L_n}} \omega_{nc}^2.\end{aligned}$$

Then the linear growth rate is easily obtained as:

$$\frac{\gamma_{Tc}}{\omega_A} = \frac{i\omega_{Tc}}{\omega_A} \simeq \frac{\gamma_{nc}}{\omega_A} \left(1 + \frac{1}{8k_{\perp}^2 L_n^2} \right).$$

This equation shows the same results as our simulations

➤ This result can be benchmarked with MINERVA code*. (a) is for constant n_0 and (b) for a profile of n_0 .



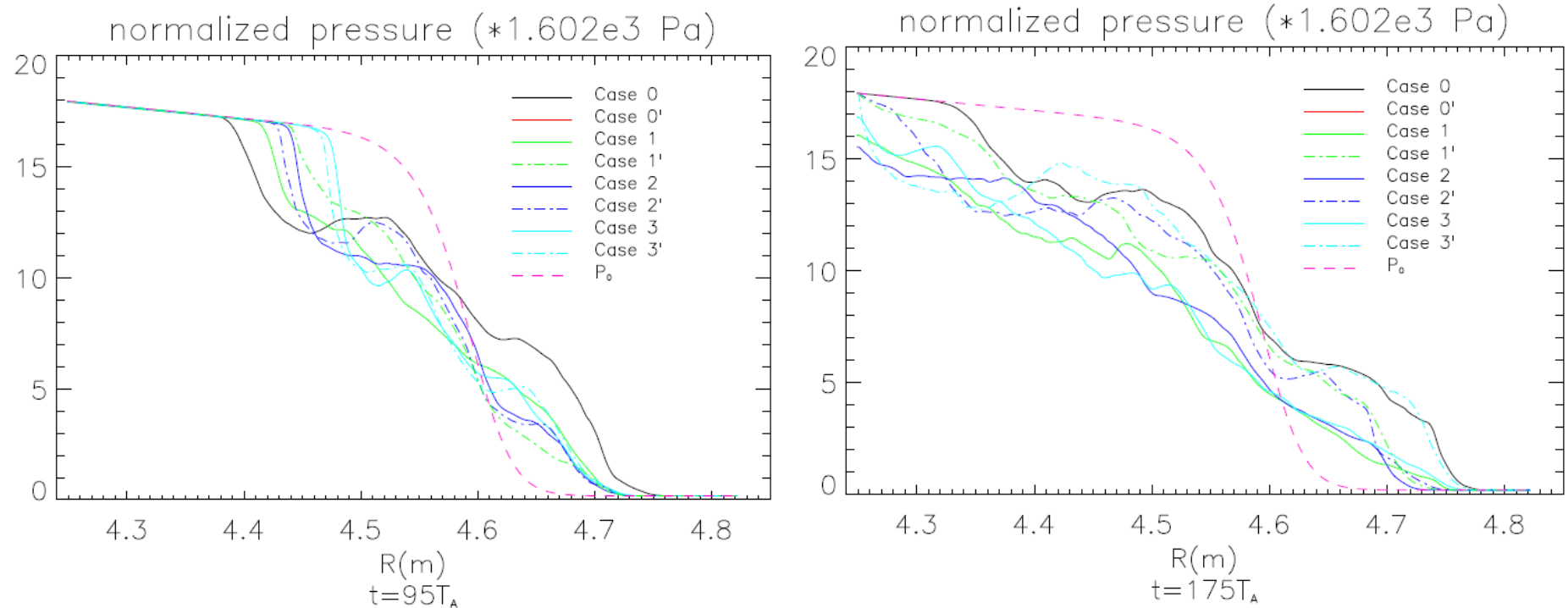
*N. Aiba, M. Furukawa, M. Hirota and S. Tokuda, Nucl. Fusion, 50 (2010) 045002.



Radial pressure profiles in nonlinear phase



Comparison of the radial pressure profiles on the outer mid-plane for the different cases for $n=15$.



➤ Case 1, 2 and 3 use Neumann BC's in the core region and 1', 2' and 3' apply Dirichlet BC's.

➤ At the early nonlinear phase. $T=95T_A$, the collapse keeps localized around the peak gradient region for all the cases. The constant n_0 case goes into the core region furthest.

➤ For all nonlinear cases, except the constant n_0 case, the perturbations go into the core boundary after roughly $t=175T_A$. This is because the cross term in the vorticity equation supplies a drive in the radial direction.

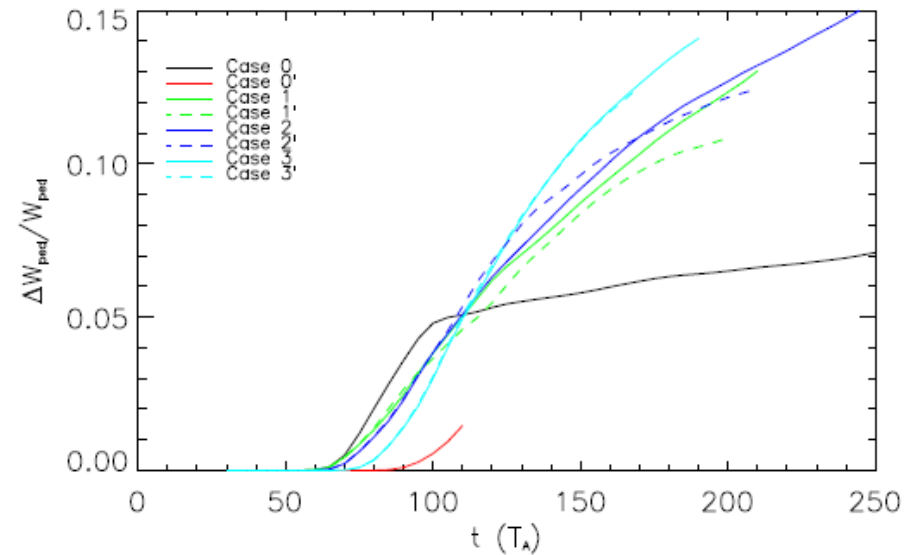
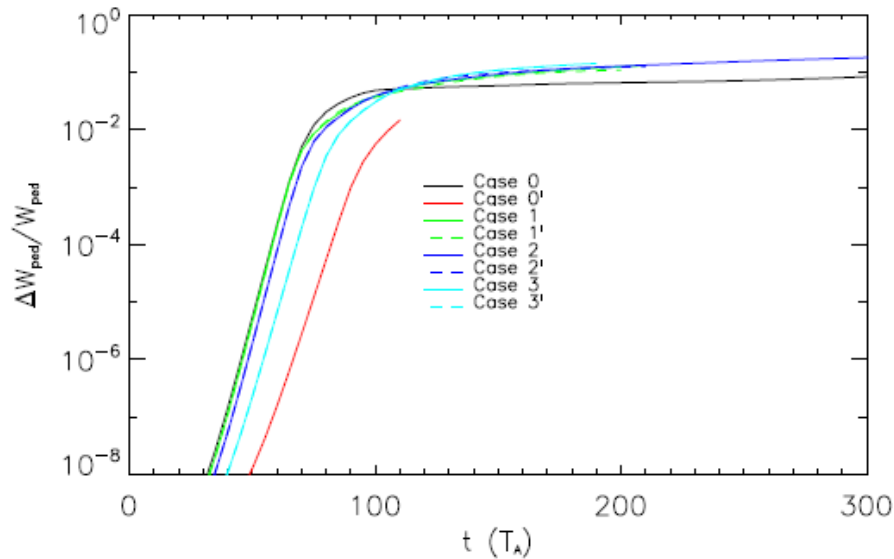


ELM size



In order to describe the nonlinear effects, we define the ELM size as

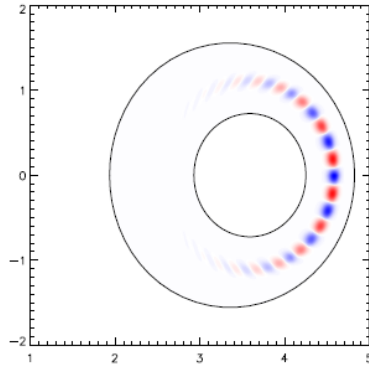
$$\Delta_{ELM}^{th} = \frac{\Delta W_{ped}}{W_{ped}} = \frac{\langle \int_{R_{in}}^{R_{out}} \oint dR d\theta (P_0 - \langle P \rangle_{\zeta}) \rangle_t}{\int_{R_{in}}^{R_{out}} \oint dR d\theta P_0},$$



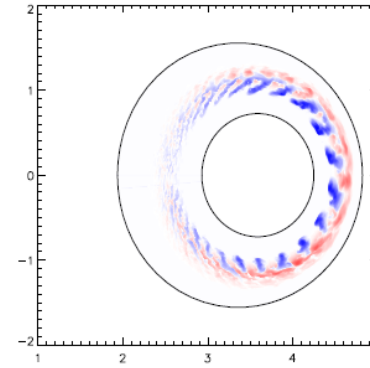
These figures show that the ELM size is larger for a gradient of n_0 than for the constant density case. This is related to the results on the previous page, that showed that the cross term in the vorticity equation supplies an additional drive in the radial direction.



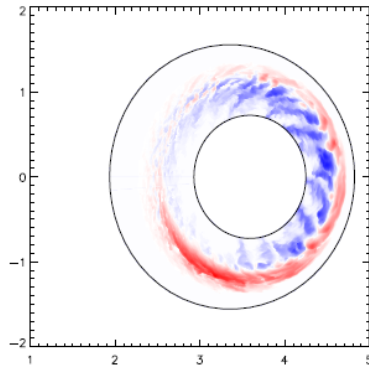
The poloidal distribution of pressure perturbation



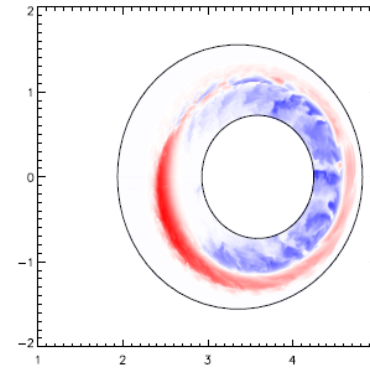
(a) $t = 0T_A$



(b) $t = 100T_A$



(c) $t = 200T_A$



(d) $t = 325T_A$

Poloidal slices in the shifted circle configuration. The density perturbations at $t = 0T_A$, $t = 100T_A$, $t = 200T_A$ and $t = 325T_A$ for Case 2 are shown here. Red colour is for a positive perturbation and blue is for a negative perturbation.



Thermal conductivity and Spitzer Resistivity



➤ Thermal conductivities:

$$\kappa_{\parallel i} = 3.9 \frac{v_{th,i}^2}{v_i}$$

$$\kappa_{\parallel e} = 3.2 \frac{v_{th,e}^2}{v_e}$$

With flux limited expressions:

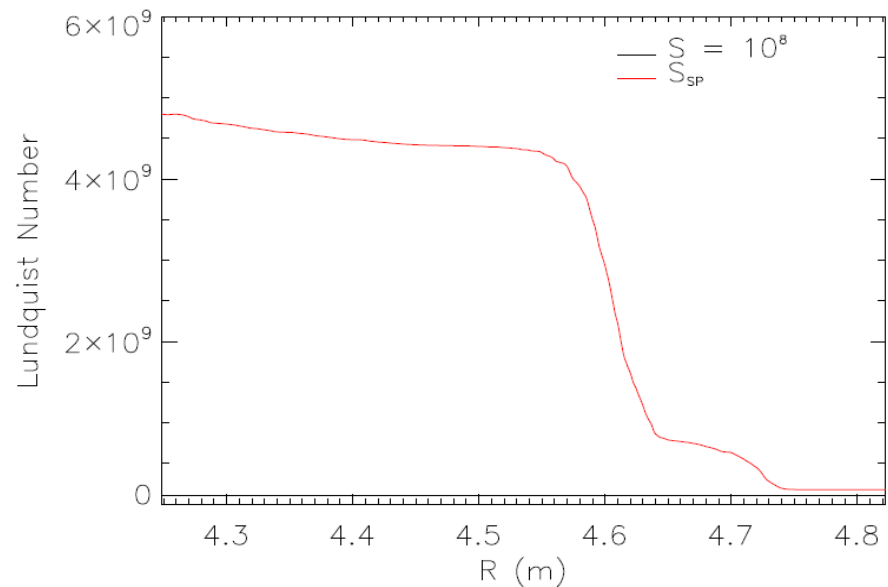
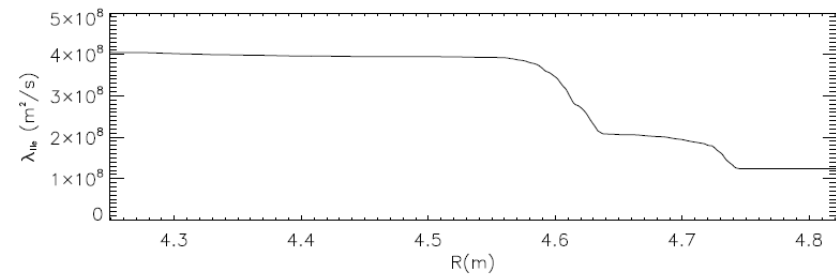
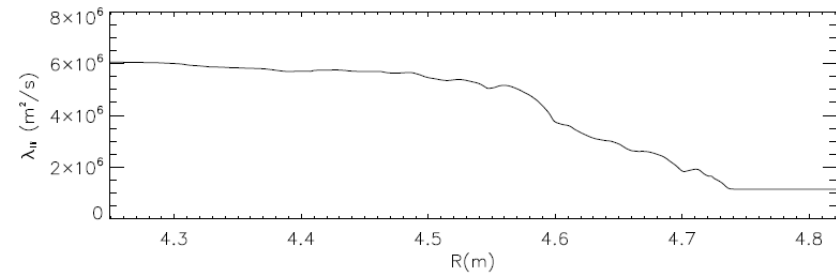
$$\kappa_{fl,j} = \frac{v_{th,j}}{q_{95} R_0}$$

Obtain the effective thermal conductivities:

$$\kappa_{\parallel j}^e = \kappa_{\parallel j} \left(\frac{1}{\kappa_{\parallel j}} + \frac{1}{\kappa_{fl,j}} \right)^{-1}$$

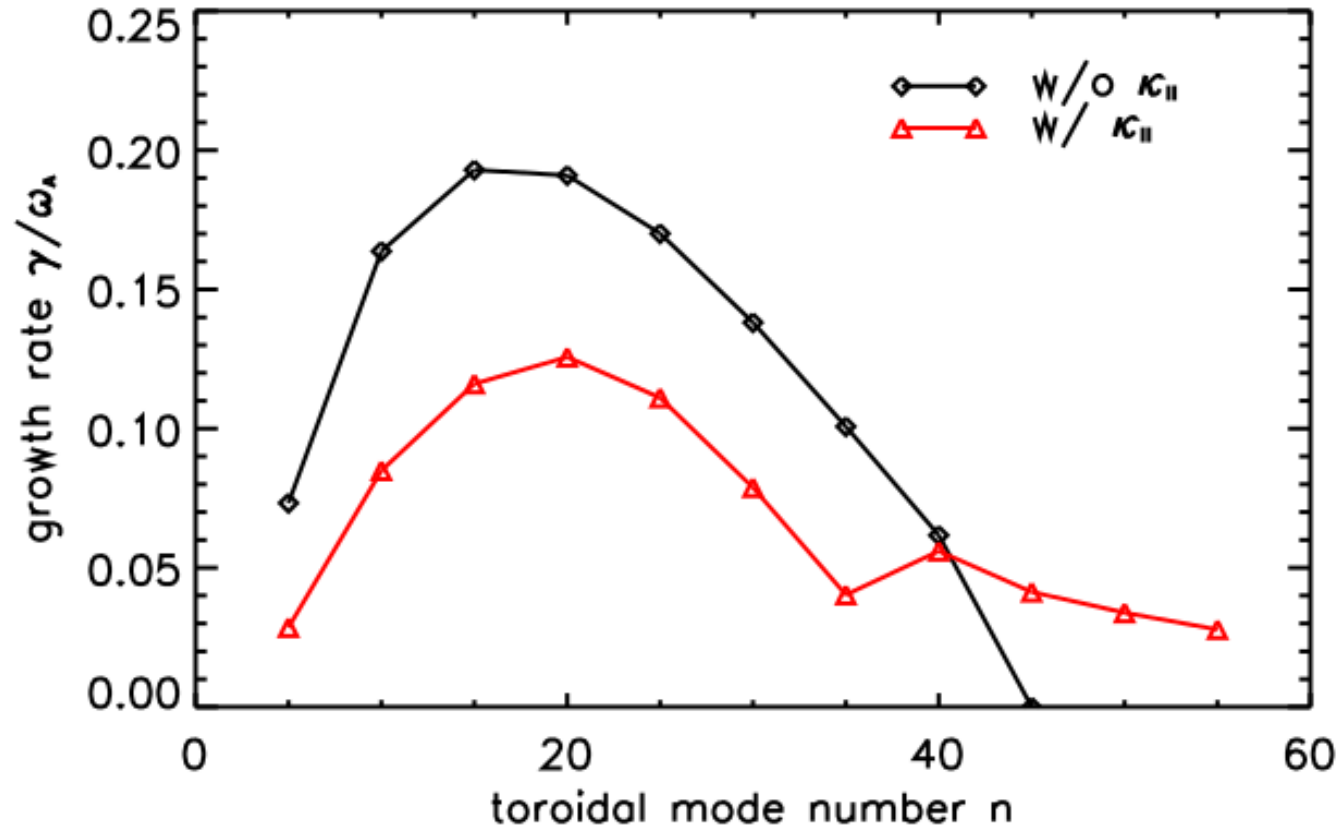
➤ Spitzer resistivity:

$$\eta_{SP} = 0.51 \times 1.03 \times 10^{-4} \ln \Lambda T^{-\frac{3}{2}}$$





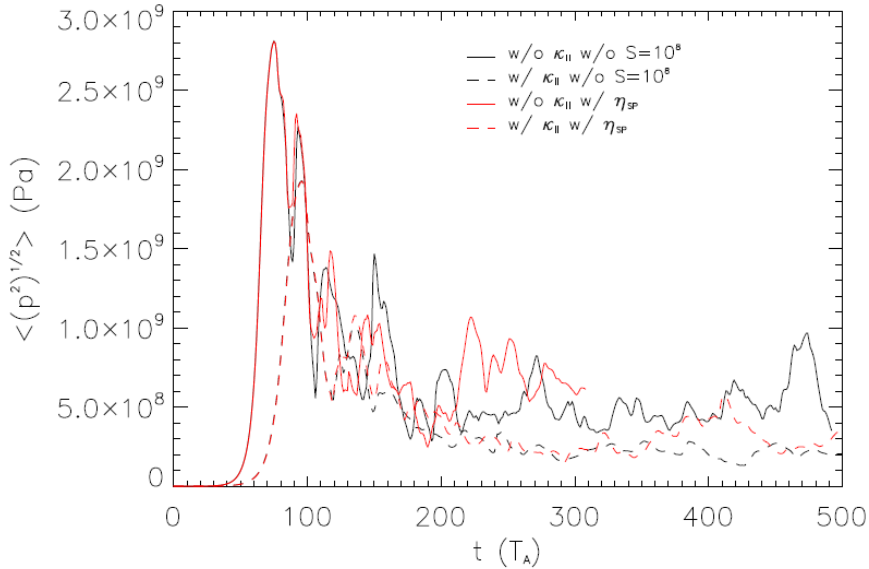
Linear effects for thermal conductivities



- For Case 2 with $\kappa_{||}$, the growth rates are decreased by 33.7% at least. The stabilizing effects are obvious.



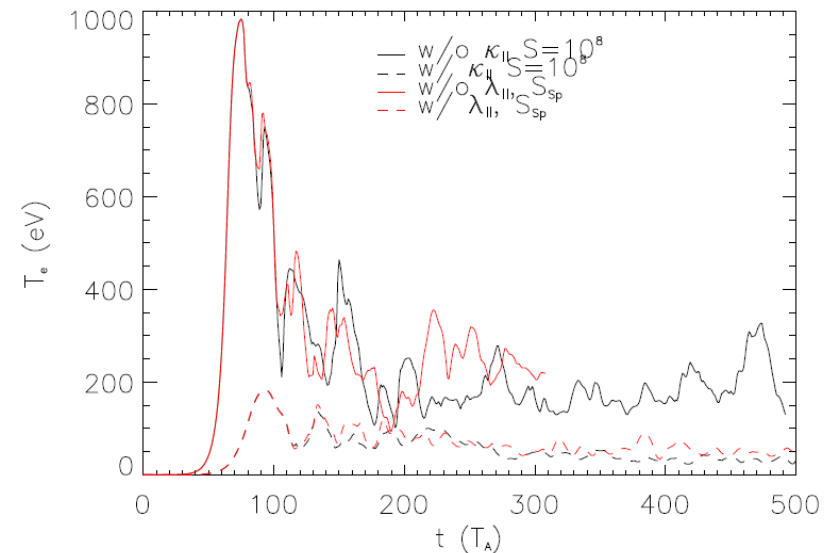
$K_{||}$ decreases the perturbations, while η_{sp} affects little



➤ The influence of η_{sp} is hard to be seen from the linear growth regime, because cbm18_dens8 is a strong ballooning instability and η_{sp} does not change too much compared with $S = 10^8$.

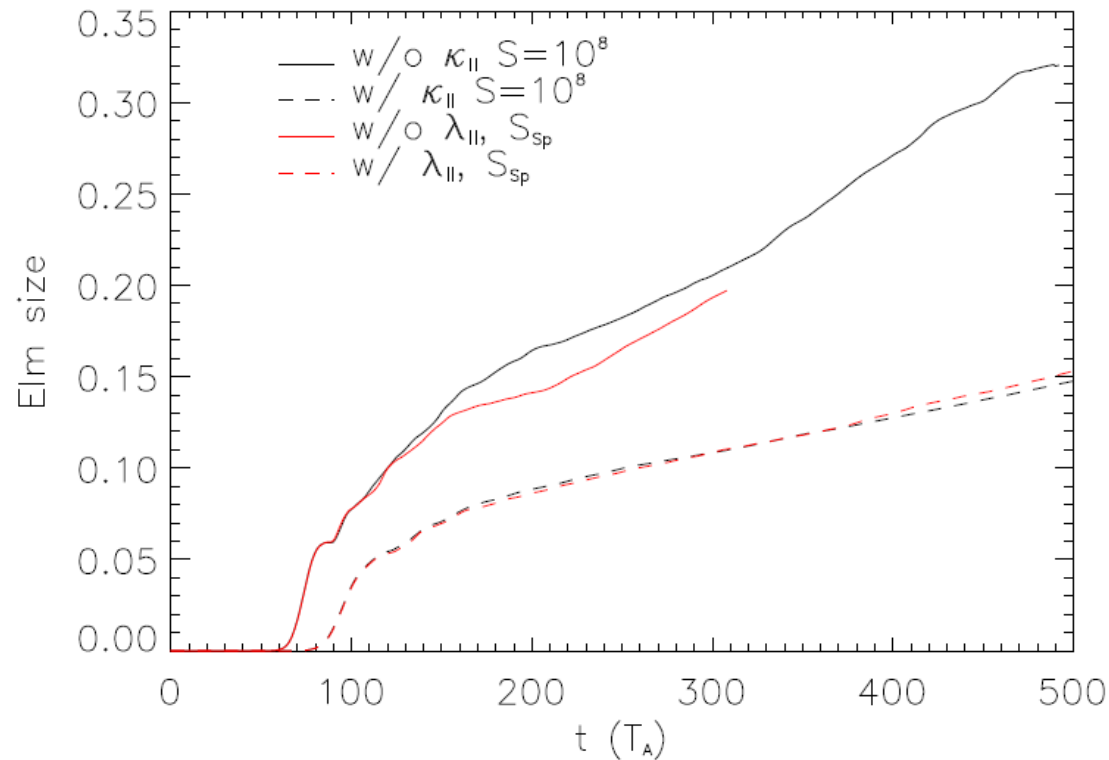
➤ Thermal conductivities damp the linear growth rate. Also the saturate value at nonlinear phase is decreased.

➤ The effects on T_e is obvious for $K_{||e}$ is much larger.





ELM size



$K_{||}$ decrease the ELM size by the ration between 44% and 54%.
 η_{sp} decreases the ELM size up to 4% before $t=320T_A$, while increase it up to 4% before $t=320T_A$ when $K_{||}$ is considered.



Time averaged radial profiles show transporting into the core region of the temperatures are stopped by $\kappa_{||}$

